Faraday Discussions

Accepted Manuscript

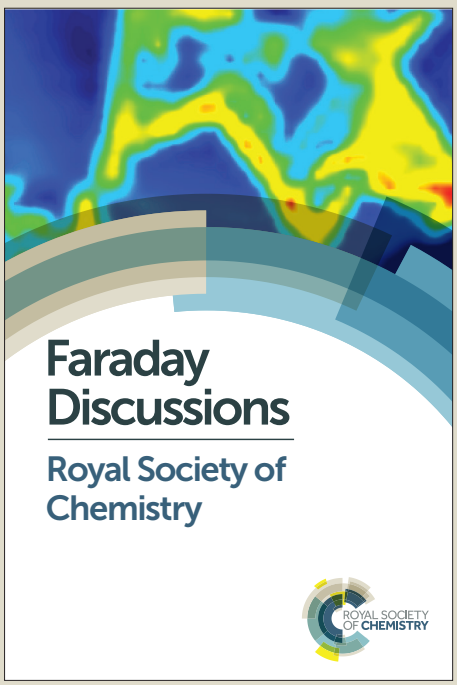

This article can be cited before page numbers have been issued, to do this please use: Y. Chiang, C. Huang, W. H. Wang and C. Chang, *Faraday Discuss.*, 2016, DOI: 10.1039/C6FD00164E.

View Article Online
DOI: 10.1039/C6FD00164E

A dual photoluminescence enhancement system: Stabilization of water soluble AIEE fluorogen using silver nanowire

Ying-Chen Chiang,[a] Chun-Ta Huang,[b] Wei Hsin Wang,[b] Cheng-Chung Chang*[c]

[a]Department of Chemical Engineering, National Chung Hsing University, Taichung 402, Taiwan

[b]Protrustech Co., Ltd, 3F.-1, No.293, Sec. 3, Dongmen Rd. East District, Tainan City 701, Taiwan

[c]Graduate Institute of Biomedical Engineering, National Chung Hsing University, Taichung 402, Taiwan

ABSTRACT

This manuscript describes the preparation of water soluble aggregation-induced emission enhancement (AIEE)-based fluorescent organic nanoparticles (FONs). The fluorescence diversity of FONs was investigated in the presence of silver nanowires. We observed that the emission of FONs can be enhanced by mixing with nanowires, which is believed to originate from the resonance between emission of FONs and surface plasmon resonances of the metal surface. That is, the AIEE phenomenon was promoted according to the metal-enhanced fluorescence (MEF) mechanism that can be used to build-up a novel double emission enhancement (DEE) platform and to extend the range of AIEE applications. The systemic fluorescence enhancement, lifetime and photostability were measured and the AIEE-MEF evaluation and the interaction between FONs and nanowires were discussed based on the obtained spectral data and SEM and fluorescent microscopy images.

DOI: 10.1039/C6FD00164E

INTRODUCTION

Nanoscale of metals exhibit remarkable optical properties due to excitation of their surface plasmons by incident light, resulting in significant enhancement of the electromagnetic field at the nanostructure surface.[1] Upon formation of the surface plasmons, metallic nanostructures can enhance the emission rates of a fluorophore; this phenomenon is known as metal-enhanced fluorescence (MEF)[2] and, usually occurs as a result of the near-field interaction between noble metal nanostructures (Ag and Au) and fluorophores.[3] MEF has become an established technology platform[4] in which metal nanostructures interact with fluorophores, leading to enhanced fluorescence, improved light resistance and reduced lifetime. Moreover, metal nanostructures have been applied to DNA, protein bioanalysis fluorescence, and tracking of cellular mechanisms and immunoassays.[5-9]

Therefore, the fluorescence intensity is usually adjusted by controlling the nanostructure size, the distance between the fluorophore and the metallic surface, and the interparticle distance.[10-14] A number of metallic nanoparticles with different shapes, such as rods, shells, rings and disks, have been synthesized chemically to achieve the desired MEF.[15-18] In addition to the metal nanoparticles, noble metal nanowires have been predicted, and in a few instances these nanowires have created an alternative surface in MEF-based applications.[19] A well-known theoretical simulations by Schatz et al.[20] showed that compared to other shapes, metal nanowires can generate much more intense electromagnetic fields at their ends and that this kind of amplification was induced by plasmon resonance in the nanowires as well as by the fact that nanowires with a high aspect ratio and sharp tips act as antennas for the radiating emission from fluorophores, making them potentially attractive substrates for MEF. Although the enhancement of fluorescence emission coupled with decreased lifetimes is important for the demonstration of the MEF phenomenon, the

DOI: 10.1039/C6FD00164E

demonstration of improved photostability of fluorophores is critical for the successful application of MEF phenomenon in biosensing and cellular imaging applications.

Fluorescent organic nanoparticles (FONs) based on aggregation-induced emission enhancement (AIEE) is another nanoscale fluorescence enhancement phenomenon. Unlike quantum dots and polymer nanoparticles, FONs are expected to play various roles in a wide variety of applications, such as optoelectronic devices, due to the flexibility of synthetic approaches for such organic small compounds. [21-25] The switching of emission properties of FONs is often size-dependent and is related to the effects of intramolecular planarization or specific intermolecular aggregation conformation. That is, in the aggregation state, intramolecular rotation is restricted and emission is thus greatly enhanced. Owing to their AIEE properties, FONs have recently emerged as novel fluorescent materials for biological sensing, imaging and cancer therapy.[26-33]

In previous studies, we have applied AIEE properties to describe the fluorescence behaviour of the solid state and water-soluble fluorogen and observed the formation of FONs, either in the spectra or intracellular localization.[34-36] We then constructed AIEE-PDT molecules that can selectively display phototoxicity to cancer cells but not to normal cells with effective ROS generation enhancement.[37, 38] In the present study, we address the build-up of a double emission enhancement (DEE) platform using of a combination of AIEE and MEF models. Here, we prepare a water soluble fluorophore 3, 7-Bis (4-aminophenyl) phenothiazine (**BAP, Fig. 1**) that exhibit low luminescence in the neutral form while emitting green fluorescence in the acidic condition based on the AIEE of the protonated BAP molecule, which is due to the formation of FONs. This pH-dependent fluorescence on/off switching was investigated in the silver nanoparticlea (AgNp) and silver nanowires (AgNw) systems. The systemic fluorescence enhancement, lifetime and photostability were measured

View Article Online
DOI: 10.1039/C6FD00164E

and the MEF evaluation and the interaction between FONs and nanostructure were discussed based on the obtained spectral data and SEM and fluorescent microscopy images.

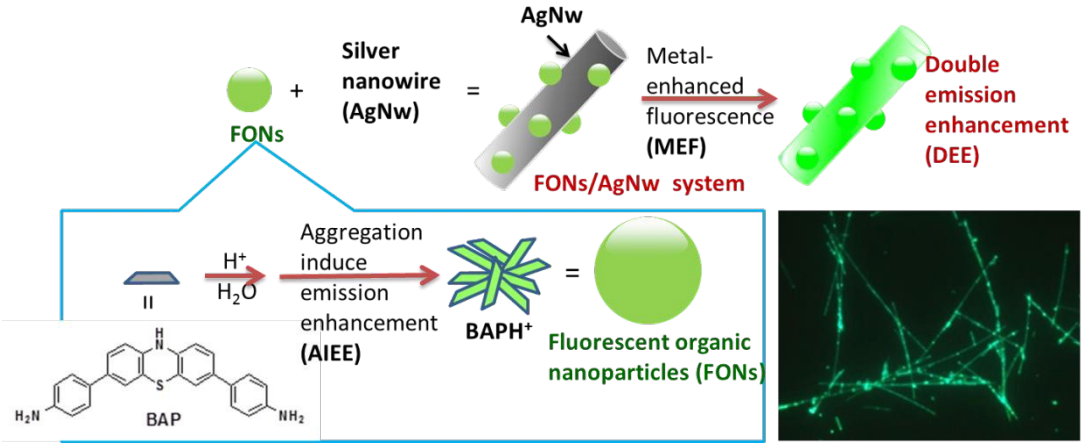

Figure 1. Structures of BAP, the formation pathway of FONs and the construction strategy of DEE based on AIEE-MEF model from FONs/AgNw system.

EXPERIMENTAL SECTION

Materials

Generally, the chemicals employed in this study were of the best analytical grade available, were obtained from Acros/ Aldrich Chemical Co. or Merck Ltd., and were used without further purification. All of the solvents used for spectral measurements were of spectrometric grade. Compound BAP was synthesized and prepared according to the procedure desvribed in a previous report.[39]

Apparatus

Absorption spectra were generated using a Thermo Genesys 6 UV-visible spectrophotometer, and fluorescence spectra were recorded using a HORIBA JOBIN-YVON Fluoromas-4 spectrofluorometer with a 1-nm band-pass in a 1-cm cell 15 length at room temperature. The SEM images of the nanostructures were obtained

View Article Online
DOI: 10.1039/C6FD00164E

using a JEOL JSM-7800F Prime Schottky field emission scanning electron microscope. An aqueous solution was deposited onto a glass. The TEM images of the nanostructures were taken on a JEOL JEM-2100F J microscope at an accelerating voltage of 100 kV. An aqueous solution that contained the compound was deposited onto a carbon-coated copper grid. The fluorescence images were taken under Leica AF6000 fluorescence microscopy with a DFC310 FX Digital colour camera. All fluorescence lifetime measurements for fluorophores and fluorophores mixed with nanostructures in solution and glass slides were performed (ProTrusTech Co., Ltd Tainan City, Taiwan.) using a RAMaker spectrometer mounted with a cooled high speed PMT detector head for photon counting (B&H) as integrated by ProTrusTech Corporation, Ltd. The spectroscopy measurements were performed using a picosecond pulse laser (405 nm) with a pulse width of 50 MHz for excitation. The fluorescence lifetimes for all samples were determined at room temperature on glass substrates. The TRPL decays at 530 nm were recorded.

Synthesis of Ag-nanoparticles (AgNp) and Ag-nanowires (AgNw)

Silver nanoparticles were synthesized according to the procedures reported in the literature.[40] Synthesis of Ag nanowires was achieved according to the procedure reported elsewhere.[41] A typical synthesis involves ethylene glycol (EG) as both the solvent and the reducing agent, with $AgNO_3$ and poly(vinvlpyrrolidone) (PVP, MW=40000) as the Ag precursor and the polymeric capping agent, respectively. In this synthesis, the $CuCl_2$ species can be added to facilitate the anisotropic growth of Ag nanowires. In a typical synthesis, 20 mL of EG were added to a disposable glass vial with a Teflon stir bar in it; the vial was then suspended in an oil bath (temperature = 150 ℃) and heated for 1 h under magnetic stirring (400 rpm). At 1 h, 160 μL of a 4 mM $CuCl_2$ solution in EG was injected into the heated EG. The solution was heated

View Article Online
DOI: 10.1039/C6FD00164E

for an additional 15 min. Next, 6 mL of a 0.147 M PVP solution in EG (concentration calculated in terms of the repeating unit) was then injected into the heated EG, followed by the addition of 6 mL of a 0.094 M $AgNO_3$ solution in EG. The colour of the reaction solution changed as follows: initially clear and colourless to yellow (within 1 min), to red-orange (within 3 min), to green, beginning to become cloudy (within 5 min), to cloudy, with a gradual shift from green to brown-red (within 30 min), and finally to opaque grey with wispiness indicating the formation of long nanowires (within 1 to 1.5 h). Upon formation of Ag nanowires, the reaction was quenched by cooling the reaction vial in a room temperature water bath. The products were washed once with acetone and three times with water in order to remove excess EG and PVP prior to the characterization.

Measurement

Preparation of FONs solution from BAP: the pKa_1 and pKa_2 values for the protonated BAP is ~5.12 and ~2.1, and the emission enhancement pH range of the BAP was pH=1-3.5.[39] Thus we directly mix certain equivalent of BAP with pH=3 dd water to make the FONs aqueous solution with certain concentration of $BAPH^+$. Here, we exclude the use of buffer solution to avoid interference from salts in performing of MEF optical measurement. **FONs/AgNw-containing thin films on glass**: mixture composed of silver nanowires and FONs were fabricated on glass in two different ways. (1) The 0, 1.5, 3 and 7.5 mg/mL concentration of Ag nanowires-containing dd water solutions 100 μL were sprayed on glass substrates to obtain variable densities of AgNw networks thin films, respectively. The solvent of Ag nanowire-deposited glass slides were then vacuum evaporated for 2 h at room temperature. Further coating of every AgNw networks thin film was made by sprinkling FONs solution (50 μM BAP in pH= 3 dd water) to fabricate layer by layer FONs/AgNw containing thin films. (2)

View Article Online
DOI: 10.1039/C6FD00164E

Similar preparing protocol but using the mixed solution of 0, 1.5, 3 and 7.5 mg/mL Ag nanowires in 50 μM BAP in pH= 3 dd water solutions (total 100 μL) to directly fabricate the mixing FONs/AgNw containing thin films. Here we prepared several FONs/AgNw containing thin films with constant concentration of FONs and variable concentration of AgNw thin films, whatever layer by layer or mixing FONs/AgNw containing thin films. These thin films were also used for SEM and microscopy analysis.

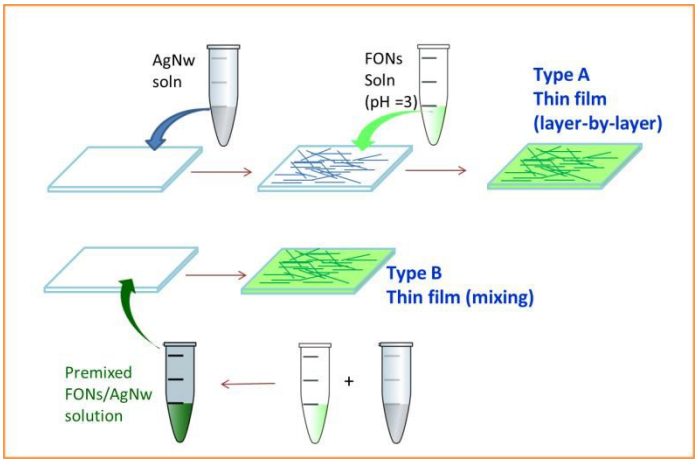

Figure 2. Two fabrication pathways for FONs/AgNw-containing thin films.

RESULTS AND DISCUSSION

In a previous study, we described the convenient preparation of 3, 7-diaryl-substituted 10H-phenothiazines **BAP**. The optical properties of protonated, deprotonated and oxidated forms of BAP were examined and diverse spectral properties were found for this compound including (1) visible fluorophores and NIR chromophores switched on by the loss of protons at 10N–H, (2) a stable phenothiazinium product with an absorption maxima of more than 950 nm after an oxidation reaction and (3) the ability to support extra phototoxicity to cancer cells with super oxide generation. Most

DOI: 10.1039/C6FD00164E

important, compound BAP can form bright FONs based on its AIEE properties upon protonation in an acidic aqueous solution and can therefore be used as a pH biosensor.[39] As shown in **Fig. 1**, FONs are constructed from $BAPH^+$ (protonated form of BAP), and the strategy of this study is to investigate whether the AIEE-MEF double fluorescence enhancement can occur in the FONs/Ag-nanostructure system.

The silver nanoparticles and nanowires were synthesized using a solution-based polyol process.[41] **Fig. 3a** shows the absorbance spectra of AgNp and AgNw in dd water. The dominant surface plasmon resonance (SPR) peak for silver nanostructure in solution was observed to be consistent with the typical optical properties of silver nanoparticle and nanowires synthesized via the polyol process, respectively.[42] Here, we focus to study the nanowires and assign the SPR peak at 400 nm the transverse SPR mode of the AgNw,[43] and broad absorption covers the wavelength range over the visible range of emission wavelengths of most commercially available fluorophores, for MEF applications. In addition to the observations described above, the absorption spectrum of AgNw in aqueous solution displayed a broadening that can be attributed to the coupling of the SPR due to the decrease in the spacing between the nanowires. The inset of **Fig. 3a** shows the real-colour photograph of AgNp and AgNw in solution. The AgNw solution is a cloudy yellow-green, a typical colour of silver colloids with the dominant transverse SPR peak occurring at approximately 400 nm. Furthermore, the TEM and SEM results can be discussed as follows. The nanoparticle size of AgNp is ca. 60~80nm (insert in **Fig. 3a**), and **Fig. 3b, 3c** present the TEM and SEM images showing that the average values for the diameter and length of AgNw for all surfaces was 60~130 nm and 8~16 μm, respectively. The average aspect ratio (length/diameter) of the nanowires is more than 100. The thickness of the PVP coating on the nanowires was measured to be 20~25 nm on the surfaces of nanowires.

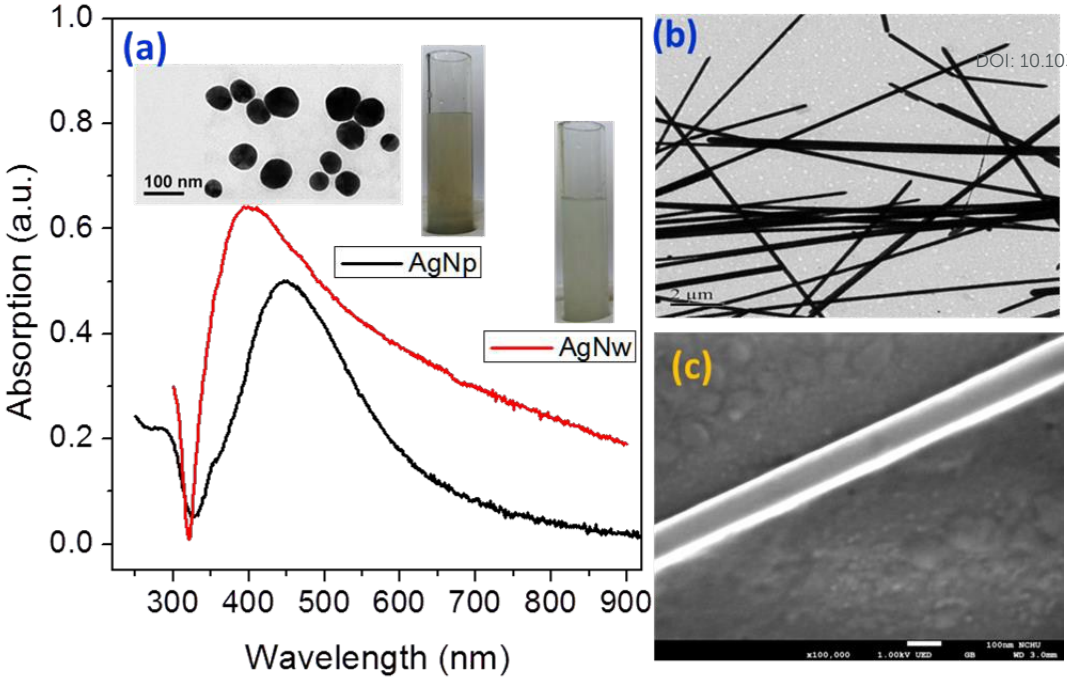

Figure 3. (a) Absorption spectra of AgNp (0.1mg/mL) and AgNw (3mg/mL), the insert shows the TEM image of AgNp and the real-color photograph of AgNp and AgNw in aqueous solution. (b) TEM image of AgNp. (c) SEM image of AgNp.

It is known that the emission enhancement of BAP can reach at least a factor of 150 in an acidic aqueous.[39] This is arises from the FONs construction due to the AIEE of protonated BAP (become $BAPH^+$). Therefore, we will examine the AIEE variation in the silver nanostructure system. First, **Fig. 4** shows absorption and emission spectra of BAP, protonated BAP ($BAPH^+$), $BAPH^+$/AgNp and $BAPH^+$/AgNp aqueous solutions corresponded to the constructions BAP, FONs, FONs/AgNp and FONs/AgNw systems. With an exception of the metal nanowires-containing solution becomes turbid and causes an apparent high spectral baseline (**Fig. 4a**). Other than the baseline problem, the absorption spectra do not exhibit large differences between these solutions. Alternatively, the fluorescence intensity of FONs/AgNw shows an almost 2-fold enhancement with respect to the free FONs system without AgNw, demonstrating the presence of an interaction between the FONs and AgNw (**Fig. 4b**).

View Article Online
DOI: 10.1039/C6FD00164E

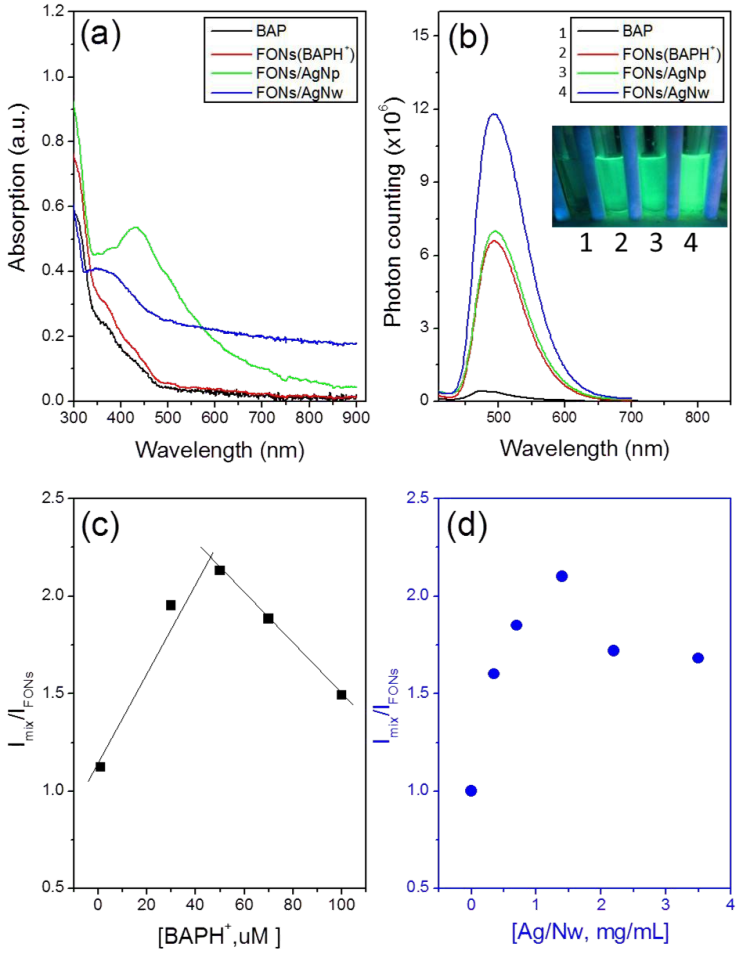

Figure 4. Absorption (a) and emission (b) spectra of BAP, protonated BAP ($BAPH^+$), $BAPH^+$/AgNp and $BAPH^+$/AgNw aqueous solutions corresponding to the BAP, FONs, FONs/AgNp and FONs/AgNw systems. (c) Emission enhanced ratios of variable concentration of BAP with respect to 1.5 mg/mL of AgNw in aqueous [pH =3]. (d) Emission enhanced ratios of variable concentration of AgNw with respect to 50uM of $BAPH^+$ in aqueous [pH =3]. I_{FONs}: emission intensities of FONs in reference aqueous without adding AgNw, I_{mix}= emission intensity of FONs in AgNw.

To find the maxima MEF effect from the AgNw to FONs, different BAP to AgNw molar ratios were examined using emission spectroscopy. By comparing between the BAP fluorescence intensities of the FONs/ AgNw and the free FONs solution, it was shown (**Fig. 4c)** the ratio of 50 uM to 1.5 mg/mL (BAP to AgNw) was optimal. Hence, we fixed the concentration of BAP (at 50 μM) and changed the equivalent of AgNw, the similar result was also observed in **Fig. 4d**. Therefore, this is

DOI: 10.1039/C6FD00164E

the phenomenon of MEF when a fluorophore in close proximity to the metal surface can emit more fluorescence via surface plasmon coupling. In this case, metal particles serve as nanoantennas to increase the local intensity of excitation light.[44,45] However, only large metal colloids with sizes larger than 0.05λ (where λ is the wavelength of the antenna operating frequency) can enhance the fluorescence of the fluorophore, and such enhancement depends largely on the distance between the fluorophore and the metal's surface.[46] The FONs/AgNw system used in the present study appeared to meet these requirements and that is why no MEF was observed for the AgNp system with FONs. Eventually, the FONs/AgNw system based on the AIEE-MEF effect can bring about a 300 fold emission enhancement with respect to the free BAP in an aqueous solution. We propose that under this condition, most FON have been contacted on the AgNw surface. This hypothesis was affirmed in **Fig. 5.**

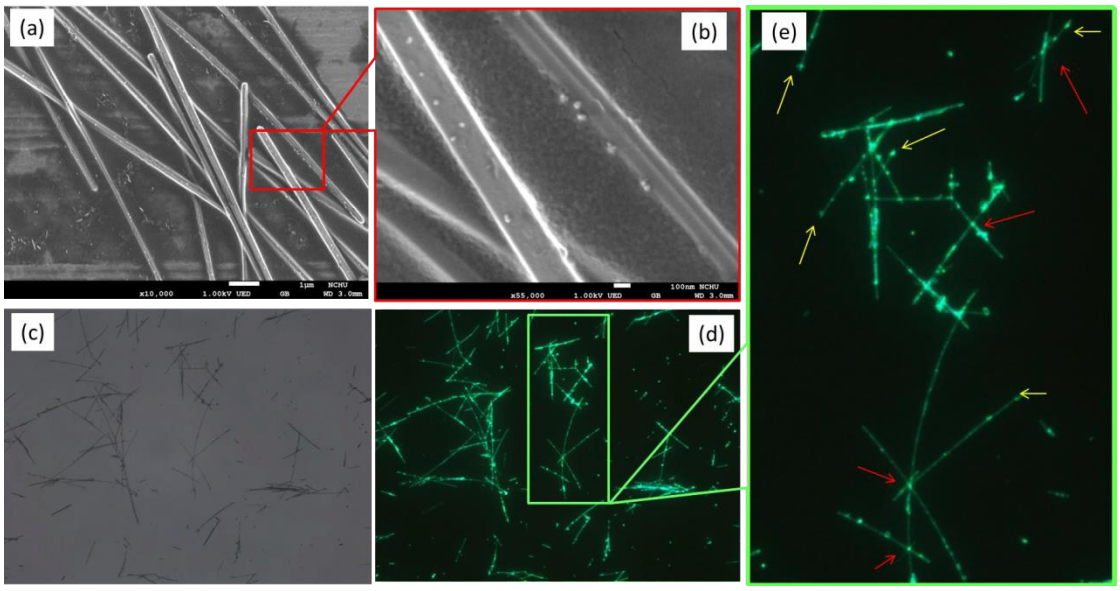

Figure 5. (a) SEM image and (b) its zoom in pattern. (c) White light image and (d) fluorescent microscopy image of FONs/AgNw system. The UV cube (ex 390/10 nm, 410 long pass filter) was used to collect the blue-green colour image. (e) Zoom in of (d).

DOI: 10.1039/C6FD00164E

To demonstrate the use of PVP modified AgNw in MEF-based applications on solid thin film platforms, these FONs/AgNw mixed solutions were deposited onto glass cover slides (type B film in **Fig.2**) for microscopy and SEM examinations. **Fig. 5a, 5b** present the SEM image obtained in the solution with the optimal ratio solution (from **Fig. 4c, 4d**). A nanoscale corn-like rod pattern with some < 20 nm size particles is clearly observed on the AgNw surface, implying that the FONs actually form under these conditions and are inferred to interact with AgNw. Meanwhile, a more exciting result is presented in **Fig. 5d** and **5e**. The entire corn nanorod was lit up by luminescence of FONs even the location of FONs on the surface of AgNw is not so concentrated. This result hints that MEF between FONs and AgNw actually occur and the photon from excited FON may resonance with surface plasma of metal and eventually, conduct to whole metal wire due to the antenna effect, as described above.

The electron microscope images in **Fig. 3b** and **5a** both show that silver nanowires form a network composed of individual wires or rods without any apparent adhesions or aggregation to each other. However, these nanowires appeared to overlap on several intersect points on the samples, which can resulted in the increased electric fields near the contact points, even for the low loading. (red arrows in **Fig. 5e**) Therefore, the fluorescence emission of fluorophores located at the contact points can be significantly enhanced because of coupling of surface plasmons, which is the superiority of the use of nanowires networks with high aspect ratio in MEF applications rather than nanoparticles. Moreover, it is known that the nanowires feature sharp ends that can be a source of additional electromagnetic field enhancement due to antenna-like concentration effect.[47] (yellow arrows in **Fig. 5e**)

The comparison of fluorescence excitation spectra of FONs/AgNw and free FONs or FONs/AgNp further confirmed that the emission intensities of FONs/AgNw were enhanced by AgNw in the entire excitation region (**Fig. 6a**). However, a

comparison to FONs/AgNp or FONs shows that a new band appeared at approximately 350 nm in the fluorescence excitation differential spectrum of FONs/AgNw (inset in **Fig. 6a**). It is known that there are several plasmon resonance peaks characteristics during the growing process of nanowire. For example, the absorptions at 350, 380, 410, and 570 nm were attributed to the plasmon resonance peaks of silver with various origins: long nanowires similar to the bulk silver, transverse mode of nanowires or nanorods, surface plasmon of nanoparticles and the longitudinal mode of nanorods.[48] This new excitation band in inset of **Fig. 6a** probably results from the resonance between the species that give rise to absorption at 360nm of BAP and the long nanowires plasmon similar to the bulk silver (peak at 350nm in **Fig. 3a**) of the metal nanostructure. This suggests that the FONs and metal absorbed the light simultaneously and then resonated the energy to produce this species.

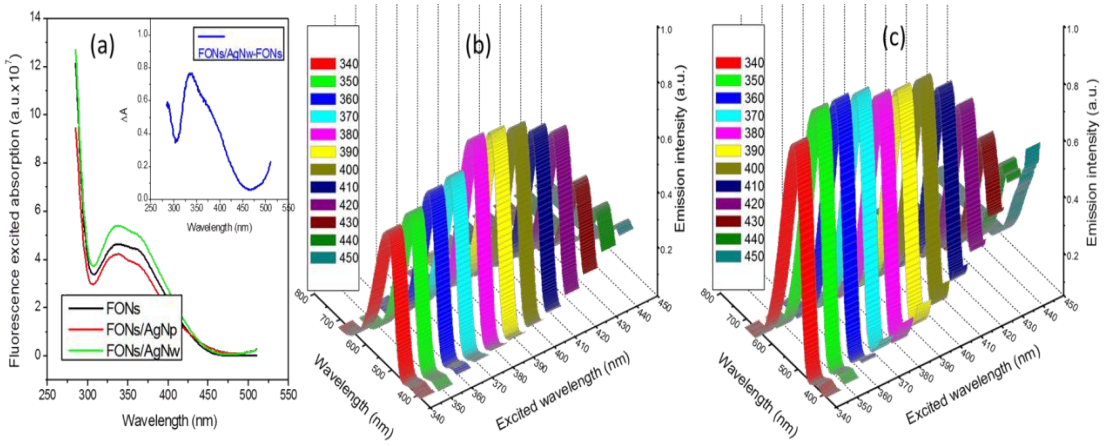

Figure 6. (a) The fluorescence excitation spectra of FONs, FONs/AgNp and FONs/AgNw, em=510 nm and insert show the differential spectrum curve between FONs and FONs/AgNw. The wavelength dependent excited (from 340~450nm, interval 10nm) emission spectra of (b) FONs and (c) FONs/AgNw system.

DOI: 10.1039/C6FD00164E

Furthermore, the emission spectra variations of **Fig. 6b** and **6c** revealed similar result. The wavelength dependent excited emission spectra of FONs indicated that the maximal emission intensity caused from exciting of 380-390 nm in aqueous solution. While the maximal emission intensity of FONs cause dominantly from exciting of 350-360 nm, in addition to exciting of 380-390 nm, in AgNw system. At this stage, we can conclude that the absorptions of FONs (360, 380nm), which overlap with the plasmon resonance peaks (350, 380 nm) of silver nanowires, and cause plasmon resonance between FONs and long nanowires bulk silver (350 nm) as well as transverse mode of nanowires (380 nm) to achieve AIEE-MEF effect.

Once the free BAP molecule was protonated, the $BAPH^+$ molecule will self-assemble to construct a positively charged FONs and consequently, to give rise to the electrostatic attraction by the PVP on the surface of AgNw. Therefore, we observed the FONs attached on surface of the AgNw in **Fig. 5**. The results of the acid titration assay presented in **Fig. 7** proved further evidence for the interaction between $BAPH^+$ and PVP. The protonation titration curve of BAP in an AgNw-containing solution shows a trend that is different from that for the FONs formation process from the protonation of free BAP. As expect, at the first half of titration, these two curves diverge to reveal that the emission intensity of the BAP mixing AgNw solution is always stronger than that of the free BAP solution due to the FONs-MEF double emission enhancement. At the last half of titration, the emission intensity of the free BAP solution system drops, implying that free FONs began to damage due to be damaged due to the second protonation of aniline group of the BAP (Pka2), while FONs from the AgNw solution appear to exhibit a more stable morphology due to the regulation of PVP.

View Article Online
DOI: 10.1039/C6FD00164E

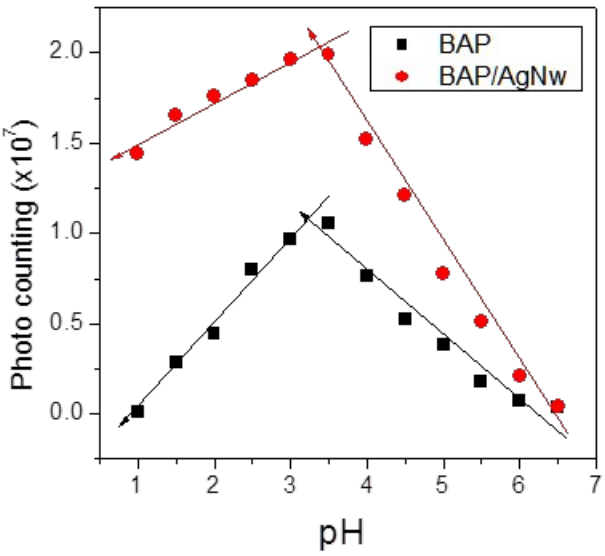

Figure 7. Intensity variation at emission =500nm from fluorescence titration spectra of BAP (become FONs) and BAP in AgNw (become FONs/AgNw) system with decreasing pH, respectively. Ex= 360 nm.

Based on the observation and discussion above, we propose that most FON have been contacted on the AgNw surface to drive the AIEE-MEF effect. Follow these inferences, the systemic emission data in **Fig. 4d** should not drop at high concentration of nanowires. However, it was observed that higher amount of AgNw make a turbid aqueous solution to cause light scattering, and deduce the emission signals. In order to observe the double emission enhancement effect directly, the effect of metal-enhanced fluorescence was studied in solid thin film by the fluorescent microscopy couple with colour CCD. That will provide more objective evidence, compare to solution condition, due to the excluding the interference and scattering. We prepared two kinds of solid thin films which sample preparing pattern shown schematically in **Fig. 2**. For the type A solid thin film, the layer-by-layer one, which was prepared by sprinkling FONs solution on a pre-coating layer of AgNW. On the other hand, for the type B solid thin film mixed sample, fabricated by mixing solutions of FONs/AgNW and spraying the mixture on a glass coverslip.

DOI: 10.1039/C6FD00164E

Fig. 8 shows the bright-field and fluorescent images of the AgNw-concentration dependent thin films and a fluorescence enhancement comparison between films type A and B. We have described that these FONs/AgNw-containing thin films were prepared with constant concentration of FONs and variable concentration of AgNw, as the photo in **Fig. 8a**. However, **Fig. 8b** and **Fig. 8c** observed the variable densities of AgNw networks thin films, which proportional to the green emission enhancement. **Fig. 8d** reveals that the fluorescence enhances more apparently in thin film B than in film A. We infer that larger fraction of FONs drop to glass but not AgNw in the low density of type A film, and then the number of the FONs contacting with the silver nanowires should be relatively fewer. Once the higher density coatings of AgNw on glass, we observed that there is no difference in fluorescence enhancement. Nevertheless, the MEF is confirmed by this protocol with increasing densities of AgNw but constant concentration of FONs, whatever layer by layer or FONs/AgNw-mixing thin films. More important, we find the emission enhancement of FONs/AgNw increase by more than 8 folds as compare to free FONs and conclude that the AIEE-MEF double emission enhancement effect in solid state is more apparent than in aqueous solution, due to the average shorter distance between the FONs and nanostructures.

View Article Online
DOI: 10.1039/C6FD00164E

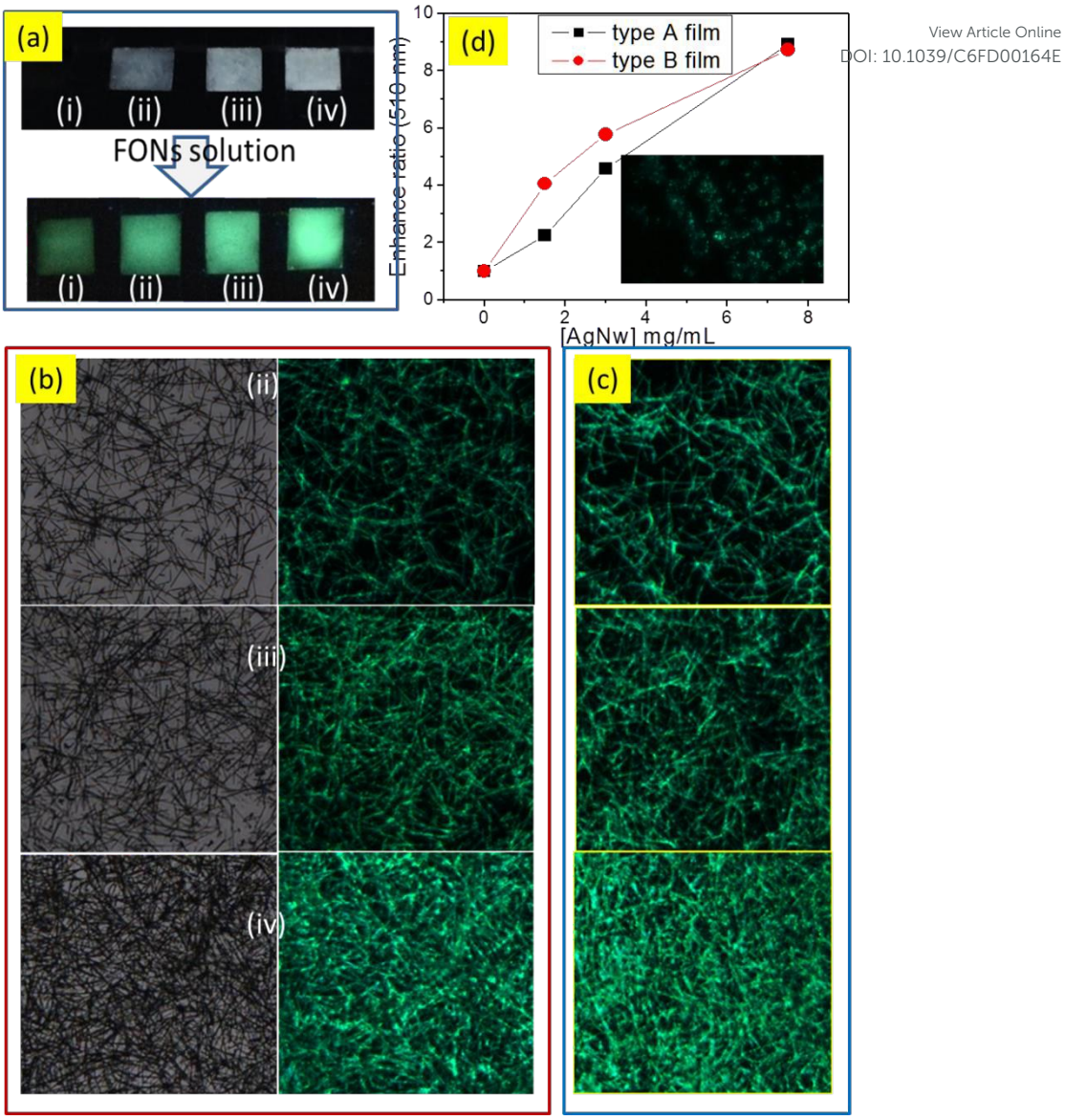

Figure 8. (a) Bright-field (up) and fluorescent (down) images of 50 μM FONs sprinkled on glass (i), (ii), (iii) and (iv) which coating (0, 1.5, 3, 7.5 mg/mL) variable densities of AgNw, respectively (type A film). (b) Bright-field (left) and fluorescent (right) images of (ii), (iii) and (iv) glass films in (a). (c) Fluorescent images of type B glass films that fabricate by spraying of FONs/AgNw mixing solutions, the contents of FONs/AgNw are 50/1.5, 50/3 and 50/7.5 (μM)/(mg/mL), respectively. (d) Quantitative emission intensities of (b) and (c) from CCD. The insert shows the fluorescent image of FONs without AgNw. The filter cube for fluorescence microscopy: ex, 390/10 nm; em, 410 nm lp filter.

In MEF-based applications, the detectability of the fluorescence emission is also affected by the lifetime and photostability of the fluorophores. In this regard, the photostability of FONs compared the FONs adsorbed onto AgNp or AgNw were investigated. **Fig. 9a** shows that the fluorescence emission of FONs decreases the

DOI: 10.1039/C6FD00164E

fastest in free form and shows the slowest decay on FONs/AgNw. Time-resolved and decay curves measured for the FONs in the appearance of nanostructures are also shown in **Fig. 9**. The black lines represent in the **Fig. 9(b)-9(g)** show the time-resolved data while the red lines are curves fitting, either biexponential for the reference or triexponential for the fluorophore-nanostructures. In the case of the reference sample, in **Fig. 9b**, the free BAP feature a biexponential decay curve with constant of 0.247 ns (97.68%) and 2.78 ns (3.32%), which represents the lifetime of most free BAP is less than 0.25 ns in aqueous, which in agreement with low emission behavior in **Fig. 4b**. For the FONs ($BAPH^+$-containing aqueous solution) and FONs/AgNp solutions we obtained two similar time-decay curves. In both cases the shorter one comparable to the reference sample and the longer one equal to approximately 2.43 ns (27.68%) and 2.93 ns (27.29%), respectively, with the higher percentage component (**Fig. 9c, 9d**). It means that the FONs seem no interacted with silver nanoparticles. On the other hand, in the case of the FONs/AgNw sample (**Fig. 9e**), triexponential analysis is suitable than biexponential, the shorter time was again comparable to the reference, while slower decay can be approximated with constants of about 2.12 ns (34.3%) and 8.86 ns (11.86%).

View Article Online
DOI: 10.1039/C6FD00164E

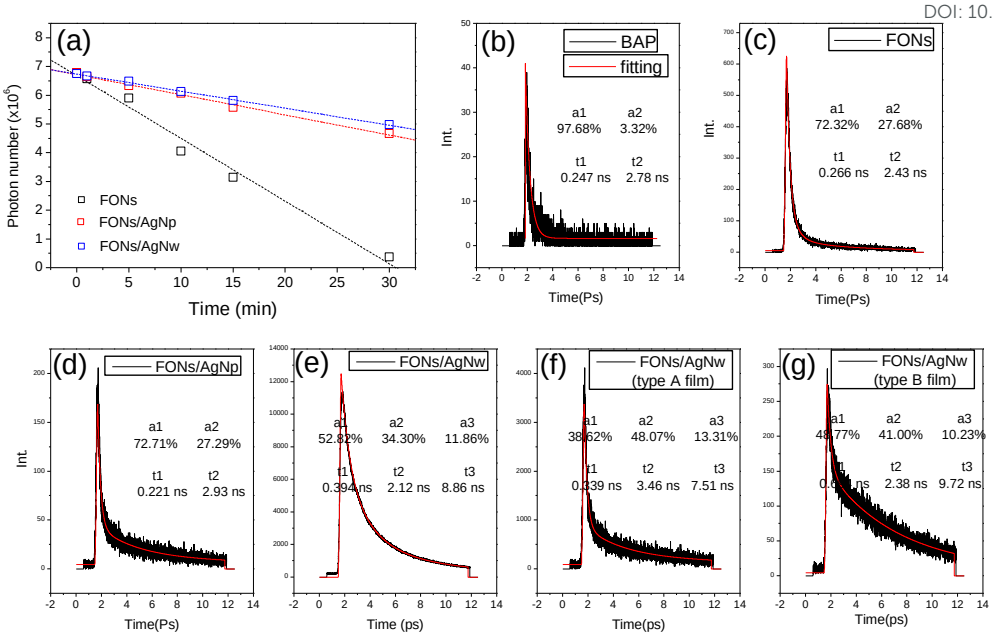

Figure 9. (a) Photostability of the FONs, FONs/AgNp and FONs/AgNw, the irradiation light source is handheld UV Lamps (6 watts). (b)-(e) Time-resolved spectra and lifetime curve fittings of the BAP, FONs, FONs/AgNp and FONs/AgNp in aqueous (pH = 3). 405 nm picosecond excitation lasers are used. (f), (g) FONs/AgNw solid film type A and B, as shown in **Fig.2**.

Consider the solution condition, the FONs may kinetically contact with nanowires and the lifetime can be increased based on two contacting model; located along the nanowires or located in the end of nanowire. It is known that the nanowires feature sharp ends that can be a source of additional electromagnetic field enhancement due to antenna-like concentration effect.[48] (yellow arrows in **Fig. 5e**) Additionally, the intersect points of nanowires, which can also resulted in the increased electromagnetic fields near the contact points and increased the SPR. (red arrows in **Fig. 5e**) These two cases with strong enhancements, the causes of longer lifetime, we observe only in a few cases using wide-field microscopy imaging of the fluorescence of the FONs/AgNw. Alternative sample preparation method, we prepare FONs/AgNw-containing solid films type A and B, to check the time decay curve. **Fig.**

DOI: 10.1039/C6FD00164E

9f, 9g show that more concrete results than in **Fig. 9e**, the component ratio of low lifetime decrease while of high lifetime increase, 3.46 ns (48.07 %) and 7.51 ns (13.31 %) for A film and 2.38 ns (41.0 %) and 9.72 ns (10.23 %) for B film, with respect to the FONs aqueous without nanowires. The promotion of the fluorescence decay time for the FONs coupled to the silver nanowires indicates that plasmon excitations in metallic nanowires influence radiative properties of the BAP in the FONs, though it is surprising that rarely lifetime enhancement in MEF cases. Nevertheless, from **Fig. 9**, these results imply that the FONs doping onto the AgNw can increase the detectability of the fluorescence emission from samples as compared to the blank.

CONCLUSION

We successfully constructed a double emission enhancement (DEE) platform based on the combination of AIEE and MEF effects. The formation of FONs from the fluorophore aggregate provided the first emission enhancement, and the MEF effect between the AgNw and FONs provided the second emission enhancement. Finally, the emission signal can be doubly promoted in order to increase the systemic detection limit. Based on our study, the silver nanorods structures synthesized herein are readily applicable to this platform but silver nanoparticles are not applicable. The AIEE-MEF effect can be initiated due to the absorption overlapping of FONs and metal nanostructure, follow by the resonance of the photon from the fluorophore emission with the AgNw surface plasmon and conduction though the entire metal rod due to the antenna effect. This interaction between FONs and AgNw was proposed and validated by observation of nanoscale corn-like rods in the SEM image and bright nanoscale corn-like rods using fluorescent microscopy, promoting photostability and increasing lifetime. This double emission enhancement (DEE) platform should be

very useful in fluorescent analysis, microarray design and charge separation in solar cells.

View Article Online
DOI: 10.1039/C6FD00164E

Acknowledgements

This work was supported financially by the Ministry of Science and Technology (MOST 104-2119-M-005 -007 -MY3) of Taiwan.

Notes and references

‡ Footnotes relating to the main text should appear here. These might include comments relevant to but not central to the matter under discussion, limited experimental and spectral data, and crystallographic data.

View Article Online
DOI: 10.1039/C6FD00164E

REFERENCE

1. R. Bardhan, N. K. Grady, J. R. Cole, A. Joshi and N.J. Halas, *ACS Nano.*, 2009, **3**, 744-752.

2. A. Li, J. Liu, G. Liu, J. Zhang and S. Feng, *J. Polym. Sci., Part A: Polym. Chem.*, 2004, **52**, 87-95.

3. S. T. Selvan, T. Hayakawa and M. Nogami, *J. Phys. Chem. B*, 1999, **103**, 7064-7067.

4. K. Aslan, I. Gryczynski, J. Malicka, E. Matveeva, J. R. Lakowicz, C. D. Geddes, *Curr. Opin. Biotechnology*, 2005, **16**, 55-62

5. Q. Huang, Z. Huang, G. Meng, Y. Fu and J. R. Lakowiz, *Chem. Commun.*, 2013, **49**, 11743-11745.

6. Y. Fu, J. Zhang, K. Nowaczyk and J. R. Lakowicz, *Chem. Commun.*, 2013, **49**, 10874-10876.

7. M. V. Y. Toshchakov, H. Szmacinski, L. A. Couture, J. R. Lakowicz and S. N. Vogel, *J Immunol.*, 2011, **186**, 4819-27.

8. J. Zhang, Y. Fu, G. Li, K. Nowaczyk, R. Y. Zhao and J. R. Lakowicz, *Res. Biochem. Biophys. Res. Commun.*, 2010, **400**, 111-6.

9. H. Szmacinski, K. Ray and J. R. Lakowicz, *Anal. Biochem.*, 2009, **385**, 358-64.

10. W. Weimer and M. Dyer, *Appl. Phys. Lett.*, 2001, **79**, 3164-3166.

11. R. Gupta, M. Dyer and W. Weimer, *J. Appl. Phys.*, 2002, **92**, 5261-5271.

12. K. Li, M. I. Stockman and D. J. Bergman, *Phys. Rev. Lett.*, 2003, **91**, 227402.

13. S. H. Guo, S. J. Tsai, H. C. Kan, D. H. Tsai, M. R. Zachariah and R. J. Phaneuf, *Adv. Mater.*, 2008, **20**, 1424-1428.

14. S. Enoch, R. Quidant and G. Badenes, *Opt. Express*, 2004, **12**, 3422-3427.

15. R. Bardhan, N. K. Grady, J. R. Cole, A. Joshi and N. J. Halas, *ACS Nano.*, 2009, **3**, 744-752.

16. S. Lal, N. K. Grady, J. Kundu, C. S. Levin, J. B. Lassiter and N. J. Halas, *Chem. Soc. Rev.*, 2008, **37**, 898-911.

17. J. Zhang, Y. Fu and J. R. Lakowicz, *J. Phys. Chem. C*, 2009, **113**, 19404-19410.

18. F. Tam, G. P. Goodrich, B. R. Johnson and N. J. Halas, *Nano Lett.*, 2007, **7**, 496-501.

19. E. M. Goldys, K. Drozdowicz-Tomsia, F. Xie, T. Shtoyko, E. Matveeva, I. Gryczynski and Z. Gryczynski, *J. Am. Chem. Soc.*, 2007, **129**, 12117-12122.

20. E. Hao and G. C. Schatz, *J. Chem. Phys.*, 2004, **120**, 357-66.

21. J. Luo, Z. Xie, J. Y. Lam, L. Cheng, H. Chen, C. Qiu, H. S. Kwok, X. Zhan, Y. Liu, D. Zhu and B. Z. Tang, *Chem. Commun.*, 2001, 1740-1741.

22. B. K. An, S. K. Kwon, S. D. Jung and S. Y. Park, *J. Am. Chem. Soc*., 2002, **124**, 14410-14415.

23. D. Xiao, L. Xi, W. Yang, H. Fu, Z. Shuai, Y. Fang and J. Yao, *J. Am. Chem. Soc.*, 2003, **125**, 6740-6745.

24. Y. Y. Sun, J. H. Liao, J. M. Fang, P. T. Chou, C. H. Shen, C. W. Hsu and L. C. Chen, *Org. Lett.*, 2006, **8**, 3713-3716.

25. S. S. Palayangoda, X. Cai, R. M. Adhikari and D. C. Neckers, *Org. Lett.*, 2008, **10**, 281-284.

26. H. Shi, R. T. K. Kwok, J. Liu, B. Xing, B. Z. Tang and B. Liu, *J. Am. Chem. Soc*., 2012, **134**, 17972-17981.

27. S. Samanta, S. Goswami, M. N. Hoque, A. Ramesh and G. Das, *Chem. Commun.*, 2014, **50**, 11833-11836.

28. X. Li, K. Ma, S. Zhu, S. Yao, Z. Liu, B. Xu, B. Yang and W. Tian, *Anal. Chem.*, 2014, **86**, 298-303.

29. Y. Li, H. Yu, Y. Qian, J. Hu and S. Liu, *Adv. Mater*., 2014, **26**, 6734–6741.

30. E. Zhao, H. Deng, Y. Hong, C. W. T. Leung, J. W. Y. Lam and B. Z. Tang, *Chem. Commun.*, 2014, **50**, 14451–14454.

31. F. Hu, Y. Huang, G. Zhang, R. Zhao, H. Yang and D. Zhang, *Anal. Chem.*, 2014, **86**, 7987–7995.

32. Y. Yuan, R. T. K. Kwok, B. Z. Tang and B. Liu, *J. Am. Chem. Soc.*, 2014, **136**, 2546–2554.

33. R. T. K. Kwok, C. W. T. Leung, J. W. Y. Lam and B. Z. Tang, *Chem. Soc. Rev.*, 2015, **44**, 4228-4238.
View Article Online
DOI: 10.1039/C6FD00164E

34. H. H. Lin and C. C. Chang, *Dyes. Pigments*, 2009, **83**, 230-236.

35. S. Y. Su and C. C. Chang, *J. Mater. Chem.*, 2010, **20**, 865-8.

36. H. H. Lin and C. C. Chang, *Org. Biomol. Chem.*, 2007, 7, 2036-9.

37. C. C. Chang, M. C. Hsieh, J. C. Lin and T. C. Chang, *Biomaterials*, 2013, **33**, 897-906.

38. Y. C. Chan, J. W. Chan, S. Y. Su and C. C. Chang, *J. Mater. Chem. B*, 2013, **1**, 2350-2357.

39. T. S. Hsieh, J. Y. Wu and C. C. Chang, *Dyes. Pigments*, 2015, **112**, 34-41.

40. A. Zielinska, E. Skwarek, A. Zaleska, M. Gazda and J. Hupka, *Procedia Cemistry*, 2009, **1**, 1560-1566.

41. W. Zhang, P. Chen, Q. Gao, Y. Zhang and Y. Tang, *Chem. Mater.*, 2008, **20**, 1699-1704.

42. M. S. Goh, Y. H. Lee, S. Pedireddy, I. Phang, W. W. Tjiu, J. M. R. Tan, X. Y. Ling, *Langmuir*, 2012, **28**, 14441-14449.

43. Y. Sun, *J. Phys. Chem. C*, 2010, **114**, 2127-2133.

44. R. M. Dickson and L. A. Lyon, *J. Phys. Chem. B*, 2000, **104**, 6095–6098.

45. G. W. Bryant, F. J. G. de Abajo and J. Aizpurua, *Nano Lett*, 2008, **8**, 631–636.

46. M. Swierczewska, S. Lee and X. Chen, *Phys. Chem. Chem. Phys.*, 2011, **13**, 9929–9941.

47. D. Kowalska, B, Krajnik, M, Olejnik, M, Twardowska, N, Czechowski, E, Hofmann and S, Mackowski1, *The ScientificWorld Journal*, 2013, Volume **2013**, Article ID 670412, 12 pages.

48. Y. Sun, B. Gates, B. Mayers and Y. Xia, *Nano Lett.*, 2002, **2**, 165-168.